35th Annual International Conference of the IEEE EMBS
Osaka, Japan, 3 - 7 July, 2013

Finite Element Modeling of Scattered Electromagnetic waves for Stroke Analysis

N.Priyadarshini, E.R.Rajkumar

Abstract— **Stroke has become one of the leading causes of mortality worldwide and about 800 in every 100,000 people suffer from stroke each year. The occurrence of stroke is ranked third among the causes of acute death and first among the causes for neurological dysfunction. Currently, Neurological examinations followed by medical imaging with CT, MRI or Angiography are used to provide better identification of the location and the type of the stroke, however they are neither fast, cost-effective nor portable. Microwave technology has emerged to complement these modalities to diagnose stroke as it is sensitive to the differences between the distinct dielectric properties of the brain tissues and blood. This paper investigates the possibility of diagnosing the type of stroke using Finite Element Analysis (FEA). The object of interest is a simulated head phantom with stroke, created with its specifying material characteristics like electrical conductivity and relative permittivity. The phantom is then placed in an electromagnetic field generated by a dipole antenna radiating at 1 GHz. The FEM forward model solver computes the scattered electromagnetic field by finding the solution for the Maxwell's wave equation in the head volume. Subsequently the inverse scattering problem is solved using the Contrast Source Inversion (CSI) method to reconstruct the dielectric profile of the head phantom.**

Keywords— **Stroke diagnosis, Microwave imaging, Finite Element Modeling, Maxwell's wave equation.**

I. Introduction

Stroke also known as Cerebrovascular Accident (CVA), is a condition in which the blood flow to a part of the brain is stopped. This is caused either by rupture of an artery leading to a shemorrhagic stroke or obstruction to the blood flow in the brain causing ischemic stroke. If the blood flow is blocked for more than a few seconds the brain cells start to die due to lack of oxygen leading to a permanent damage. Ischemic stroke accounts for 50% - 85% of all strokes worldwide [1] and in India about 50% to 85% of stroke is Ischemic and 7% - 27% accounts for hemorrhagic stroke [2]. Both of these conditions are fatal unless treated right away to return the blood flow to deprived areas and restore neurological functions.

The preliminary diagnosis for the stroke is done by physical and neurological examination backed up by the data from Computer Tomography (CT), Magnetic Resonance Imaging (MRI), Ultrasound or Arteriography. The MRI or CT scans would give us an accurate result to recognize the blood clot, to to localize the stroke and to date the level of progression. These processes are however costly and time-consuming when the growth of stroke is continuously monitored.

Microwave Tomography (MWT) for detecting and analyzing brain anomalies has been recently proposed to complement the current diagnosing modalities. The three major advantages of MWT over the existing modalities are, one being able to perform continuous monitoring as microwaves are non ionizing radiations unlike CT, the second being the property of the affected tissue showing variation in its dielectric values from the healthy tissues and the third being portable and cost effectiveness of the design [3]. MWT is based on the principle that the occurrence of stroke would create a pool of blood or clot with decreased oxygenation of the tissues that alter the dielectric properties of the tissues compared to that of the healthy brain [4]. Hence when the brain tissues are exposed to low levels of electromagnetic energy at microwave frequencies generated from different transmitter locations around the head, the scattered electromagnetic fields can be measured. From the acquired data the imaging could be made possible using the Contrast Source Inversion (CSI) method to reconstruct the dielectric profiles of the significant scatters.

II. Methodology

A. Phantom Head Model

The head phantom with hemorrhagic stroke and ischemic stroke was simulated by approximating the internal structural layers as ellipses shown in Fig. 1. The dielectric properties mainly the conductivity (σ) and the relative permittivity (ε_r) for the different layers of the normal head at 1 GHz are got from a published data [5,6] and are presented in Table 1. Improved spatial resolution could be got at higher frequencies, however as the frequency increases the attenuation of the signal by the biological tissues also increase leading to reduced penetration depth. From [5] the attenuation was found to be very high between 1GHz to 2GHz and hence a frequency between 0.5GHz and 1GHz was suggested to be optimal for brain imaging.

The relative complex permittivity of a lossy material is given by (1), which depends upon the frequency of radiation.

$$\acute{\varepsilon}_r = \varepsilon_r + \sigma/j\omega\varepsilon_0 \quad (1)$$

N.Priyadarshini and E.R.Rajkumar are with the Biomedical Engineering Division, School of Bio Sciences and Technology, VIT University, India (e-mail: a123priya@gmail.com, raja01aug@gmail.com, errajkumar@vit.ac.in).

In (1), $\acute{\varepsilon}_r$ is the relative complex permittivity, ε_r is the real relative permittivity, σ is the conductivity, ω is the angular frequency and ε_0 is the free-space permittivity.

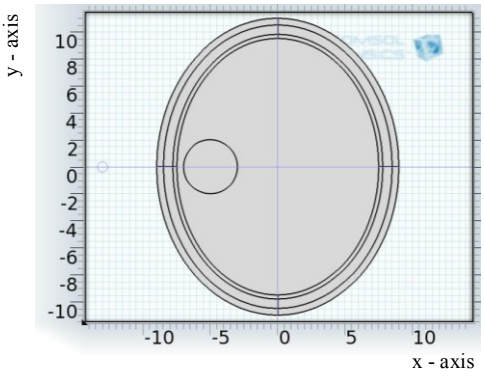

Figure 1. Brain cross sectional geometry in the *x-y* plane consisting of the hemorrhagic stroke with a radius of 2cm, grey matter, Cerebro Spinal Fluid (CSF), skull and skin from innermost to the outermost.

TABLE I
Tissue dielectric properties at 1GHz, used in the head phantom

Tissue	Thickness	ε_r	σ [S/m]
Skin	0.5cm	41	0.89977
Skull	0.7cm	12	0.15566
CSF	0.3cm	68	2.4552
Grey Matter	-	52	0.98541
Ischemic Stroke	-	36	0.15
Hemorrhagic Stroke	-	61	1.5829

The frequency dependence of the complex relative permittivity values governed by the Cole-Cole expression is given in (2) and the frequency dispersive nature of these biological tissues [6] due different frequencies ranging from 500MHz to 2GHz is shown in Fig.2

$$\acute{\varepsilon}(\omega) = \varepsilon_\infty + (\varepsilon_s - \varepsilon_\infty)/(1 + (j\omega\tau)^{1-\alpha}) + \sigma/(j\omega\varepsilon_0) \quad (3)$$

Here ε_∞ is the permittivity at frequencies where $\omega\tau >> 1$, ε_s is the permittivity at $\omega\tau << 1$, α is the dispersion parameter and τ is the mean relaxation time.

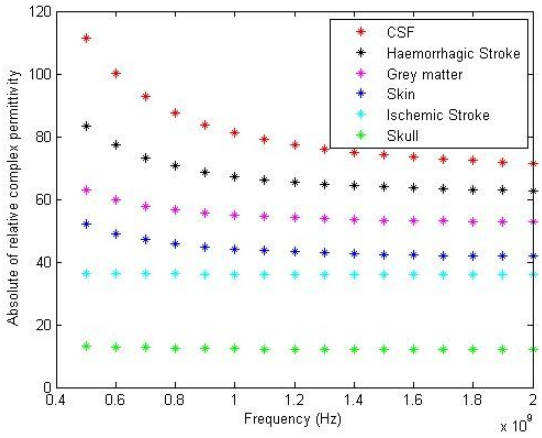

Figure 2. Absolute value of relative complex permittivity vs Frequency (Hz) in human head tissues.

Spatial resolution of the imaging could be improved at higher frequencies of microwaves, however the attenuation of the EM field in biological media also increases which decrease the Signal-to-noise (SNR) ratio. From [9] the highest frequency at which the signals are detected with a reliable SNR and not compromise for the imaging resolution was taken as 1GHz.

The transmitter a half wave dipole antenna was designed for a wavelength (λ) of 30 cm using a cylinder of radius $\lambda/80$. The arm length of the dipole antenna is $\lambda/4$ with the gap size of $\lambda/400$. These antennas are placed at eight locations equidistant with the adjacent one in an elliptical array around the simulated head phantom. When one antenna is transmitting the microwaves the rest are in the receiving mode and the excitation is carried out in a sequence along the elliptical array. The Perfectly Matched Layer (PML) is designed as the outermost sphere with a thickness of 0.4 cm with the absorbing boundary condition. The free space enclosed by the boundary sphere forming the MWT chamber is filled with air having the dielectric values $\sigma = 0$ [S/m] and $\varepsilon_r = 1$.

B. Forward Scattering problem

The major goal of solving the forward problem is to find the scattered Electric field E_{scat} for a known contrast function χ which is derived from the dielectric values of the head given in Table 1. The incident Electric field E_{inc} is calculated in the absence of the head phantom and the total electric field E in the presence of the head phantom. The dipole antenna generates the electric field perpendicular to the transverse plane of the head causing Transverse Magnetic (TM) polarization. Using Maxwell's curl equations (4) and (5), the total electric field E in the imaging domain can be found from the computation of the vectorial wave equation (5).

$$\nabla \times E = -j\omega\mu H \quad (4)$$

$$\nabla \times H = j\omega\varepsilon E + \sigma E \quad (5)$$

Here ω, ε and σ are the angular frequency, permittivity, permeability and electrical conductivity respectively and E and H are the electric and magnetic field vectors respectively. By taking the curl of (4), the magnetic field vector H can be eliminated to from the electric field to form the double curl equation and the governing wave equation could be formed as given in (7).

$$\nabla \times (\nabla \times E) = -j\omega\mu\,(\nabla \times H) \quad (6)$$

$$\nabla \times \mu^{-1}\,(\nabla \times E) - \omega^2\,\varepsilon_0\,(\varepsilon_r - j\sigma/(\omega\varepsilon_0))\,E = 0 \quad (7)$$

The electric field vector E forms the main feature node for solving the wave equation and ∇ is the vector differential operator. The FEM solver converts the wave equation into a linear system and computes it through an iterative method to find the total and incident electric field for each of the eight transmitter locations. The analysis was performed using the linear MUMPS (**MU**ltifrontal **M**assively **P**arallel **S**parse)

which could solve for a large linear system of matrices. The iterations are set to continue until the error between successive iterations reaches a tolerance level of 0.1%. The accuracy of the solution could be increased by increasing the mesh density in the head volume upon which wave equation was solved. From [10] and [11], at least 10 linear or 5 second order elements per wavelength should be present upon meshing, for the solution to converge. The created mesh consists of about 183,357 yielding a solution solved for approximately 1,205,898 degrees of freedom.

The simulations are run for each of the eight transmitter locations placed equidistant in an elliptical array around the head. From the computed total electric field E and incident electric field E^{inc} data, the scattered electric filed E^{scat} could be computed as $E^{scat} = E - E^{inc}$.

C. Inverse Scattering Problem

In the electromagnetic inverse scattering the shape, position, dielectric properties of the object of interest could be found from the scattered electromagnetic field data got from solving the forward problem. Mathematically this MWT problem is nonlinear and ill-posed comprising a large number of unknown parameters. From [12] application of nonlinear inversion algorithms like Gauss-Newton Inversion, Newton Kantorovich or Distorted Born Iterative Method for this problem might not be practical and hence this study is performed using the Contrast Source Inversion (CSI) method which approximates the nonlinear problems into a number of linear inverse problems [13]. Moreover unlike Newton based algorithms where the solution for the forward problem is required for the each iteration of regularization, the CSI method does not need it. The algorithm presented here is from [14], where the electric field data could be expressed as scalars which reduce the computational work for a two-dimensional TM setup.

The CSI method frames the inverse problem with respect to the contrast distribution χ and the contrast source W_j defined as

$$W_j(q) = \chi(q)\, E_j(q) \quad (7)$$

E is the total electric field at the point q belonging to the imaging domain. Subscript j denotes the antenna at a particular location used in irradiating the phantom to give a distribution of the electromagnetic field. The contrast function $\chi(q)$ is given by

$$\chi(q) = k^2(q) / (k^2_{bg} - 1) \quad (8)$$

Wherein, $k^2(q) = \omega^2\mu_0\varepsilon + j\omega_0\mu_0\sigma$, is the squared complex wave number with ε and σ being the permittivity and conductivity of the brain tissues at position q. $k^2_{bg}(q) = \omega^2\mu_0\varepsilon_{bg} + j\omega_0\mu_0\sigma_{bg}$ gives the squared complex wave number of the background medium with ε_{bg} and σ_{bg} being the permittivity and conductivity of the background medium at position q. The Integral Equation Contrast Source Inversion (IE-CSI) algorithm relates the incident electric field E_{inc} which is known and the unknown total electric field E is forming a nonlinear equation given by

$$E_j(q) = E_j^{inc}(q) + k^2_{bg} \int_D G(q,q')\, E_j(q')\, \chi(q')\, dq' \quad (9)$$

In (9) G is the Green's function of the background medium, (q,q') forms the position vectors in the imaging domain D upon which the integration is performed. By substituting (8), the integral equation (9) becomes

$$E_j(q) = E_j^{inc}(q) + k^2_{bg} \int_D G(q,q')\, W_j(q')\, dq' \quad (10)$$

This is called the data equation forming a linear relationship between the total electric field that could be found from the forward solver and the contrast sources in the imaging domain. Finally the values got from each of the transmitter locations are summed up to form the dielectric profile of the head phantom.

III. Results and Discussion

The MWT brain imaging was performed at 1GHz using a phantom head model simulated with hemorrhagic stroke and Ischemic Stroke modeled as a circle of radius 2cm. Linear MUMPS stationary solver was adopted to solve the forward problem using COMSOL Multiphysics and the scattered electromagnetic field is generated for each of the transmitter locations. It can also be noted that the dielectric contrast between the normal tissues and the stroke reduces when the frequency goes beyond 1GHz, and hence choosing an appropriate frequency to improve the imaging resolution is crucial. To assess the performance of the MWT method the measured electric field has been taken as a noise free data, so that preeminent results are gotten, considering that the imaging is performed under good working conditions. To evaluate the method under realistic conditions some error values could be added to the scattered electric field data that was calculated from the forward solver to represent the measured electric field. Later upon regularization the dielectric profiles could be reconstructed back with minimal change from the designed values. The spatial distribution of the normalized electric field and normalized magnetic field of hemorrhagic stroke at 1GHz is shown in Fig.3.

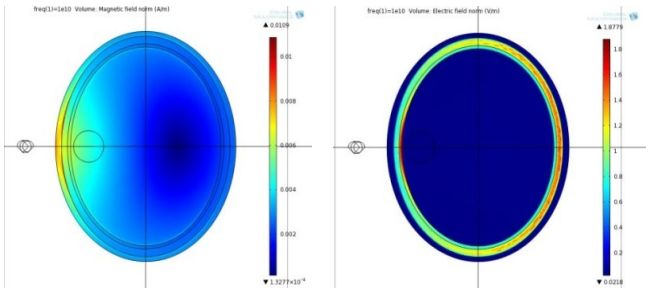

Figure 3. Spatial distributions of the normalized Magnetic field and Normalized Electric field in the head phantom with haemorrhagic stroke when the dipole antenna is radiating at 1 GHz.

The scattered data in both types of stroke vary as a function of the dielectric properties of the tissues and these values are exported from COMSOL into MATLAB to solve

for the inverse problem using CSI method from which the dielectric profiles of the simulated phantom head could be reconstructed. Fig 4 and Fig 5 provides the validation of the MWT system with the simulated hemorrhagic and ischemic stroke of radius 2 cm. The hemorrhagic stroke shows a different dielectric property than Ischemic when radiated with microwave frequencies.

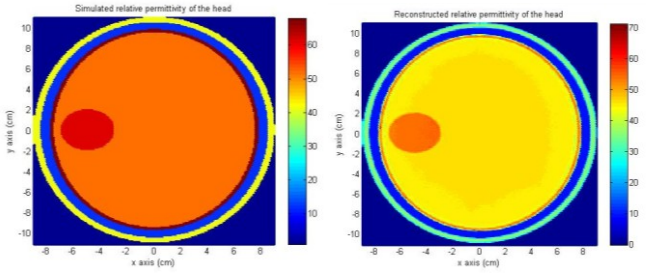

(a) (b)

Figure 4. Validation of the MWT imaging method: (a) Simulated Relative Permittivity (b) Reconstructed Relative Permittivity, of the head phantom with hemorrhagic stroke using the CSI method under ideal conditions.

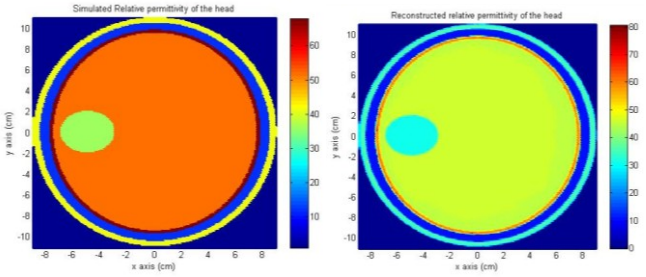

(a) (b)

Figure 5. Validation of the MWT imaging method: (a) Simulated Relative Permittivity (b) Reconstructed Relative Permittivity, of the head phantom with ischemic stroke using the CSI method under ideal conditions.

No priori information except the dielectric properties of the background medium was taken into consideration. The relative permittivity of the hemorrhagic stroke was found as $\varepsilon_r = 55.64712$ and for Ischemic stroke as $\varepsilon_r = 31.34166$ after reconstruction under ideal conditions. This study is a preliminary step in showing that this method could be considered for further studies in microwaves for diagnosis and continuous monitoring of brain stroke.

IV. Conclusion

Microwave Tomography could be used for predicting the unknown geometrical parameters like size, location and dielectric properties of the head from the scattered EM field data. The notable contrast in the tissue dielectric properties offered a significant advantage for the purpose of diagnosing between Hemorrhagic and Ischemic strokes. Since the problem posed a non linearity simple inversion method like the Contrast Source Inversion method was used. The FEA results give evidence that the microwaves could be used in analyzing the stroke from which progressive growth or recurrence could be monitored.

References

[1] Fiona C Taylor, Suresh Kumar K, Stroke in India Factsheet, South Asia Network for Chronic Disease, IIPH Hyderabad, Public Health Foundation of India, 2012.

[2] Mishra NK, Khadilkar SV. Stroke program for India. Ann Indian Acad Neurol 2010; pp: 28-32.

[3] R. Scapaticci, L. Di Donato, I. Catapano and L. Crocco L, A Feasibility study on Microwave Imaging for Brain Stroke Monitoring, Progress In Electromagnetics Research B, 2012, Vol. 40, pp: 305-324.

[4] D. Ireland and M. Bialkowski, Microwave head imaging for stroke detection, Progress in Electromagnetics Research M, 2011, Vol. 21, pp: 163-175.

[5] Serguei Y. Semenov and Douglas R. Corfield, Microwave Tomography for Brain Imaging: Feasibility Assessment for Stroke Detection, Journal of Antennas and Propagation, Volume 2008, Article ID 254830. doi:10.1155/2008/254830.

[6] Jozef Surda, Elena Cocherova, Oldrich Ondracek, Tissue Parameters Influence on the Microwave Energy Absorption in Biological Objects, 14th Conference on Microwave Techniques, 2008, pp. 1 – 4

[7] Tobias Meyer, Microwave Imaging of High-Contrast Objects. Otto-von-Guericke Universitat Magdeburg: 2005. eBook.

[8] S. Y. Semenov, R. H. Svenson, V. G. Posukh, A. G. Nazarov, Y. E. Sizov, A. E. Bulyshev, A. E. Souvorov, W. Chen, L. Kasell and G. P. Tatsis, Dielectrical spectroscopy of canine myocardium during acute ischemia and hypoxia at frequency spectrum From 100 kHz to 6 GHz, IEEE Transactions on Medical Imaging, Vol. 21, No. 6, June 2002.

[9] Dielectric properties of body tissues in the frequency range 10 Hz to100 GHz, Available: http://niremf.ifac.cnr.it/tissprop/, May 26, 2010.

[10] X.G.Li , H.von Holst, J.Ho and S.Kleiven, 3-D Finite Element Modeling of Brain Edema: Initial Studies on Intracranial Pressure Using Comsol Multiphysics, Excerpt from the Proceedings of the COMSOL Conference 2009 Milan.

[11] Abhishek Datta, Maged Elwassif and Marom Bikson, Electrical Stimulation of Brain using a realistic 3D Human Head Model: Improvement of Spatial Focality, Excerpt from the Proceedings of the COMSOL Conference 2008 Boston.

[12] Abubakar A, Habashy TM. The diagonalized contrast source inversion approach for elastic wave inversion. IEEE Transactions on Ultrasonics, Ferroelectrics, Frequency Control. 2007 Sep; 54(9):1834-40.

[13] Amer Zakaria, Colin Gilmore and Joe LoVetri, Finite-element contrast source inversion method for microwave imaging, IOP Publishing, Inverse Problems 26 (2010) 115010 (21pp).

[14] Tonny Rubaek, Paul M. Meaney and Keith D. Paulsen, A Contrast Source Inversion Algorithm Formulated Using the Log-Phase Formulation, Hindawi Publishing Corporation, International Journal of Antennas and Propagation, Volume 2011, Article ID 849894, 10 pages doi:10.1155/2011/849894.

[15] O'Halloran, M. Glavin, and E. Jones, Rotating antenna microwave imaging system for breast cancer detection, Progress In Electromagnetics Research, 2010, Vol. 107, pp: 203-217.

[16] Andreas Fhager, Mikael Persson, Stroke Detection and Diagnosis with a Microwave Helmet, 6th European Conference on Antennas and Propagation (EUCAP), 26-30 March 2012, pp: 1796 – 1798.

[17] Serguei Y. Semenov, E. Bulyshev, Vitaliy G. Posukh, Yuri E. Sizov, Alexander E. Souvorov, Peter M. van den Berg, and Thomas C. Williams, Microwave-Tomographic Imaging of the High Dielectric-Contrast Objects Using Different Image-Reconstruction Approaches, IEEE Transactions on Microwave Theory and Techniques, Vol. 53, No. 7, July 2005.